



Impact of High Strength Rebars on Seismic Behavior of Lightly Reinforced Boundary Elements

S. Sharifi, S. Tariverdilo*, C. Gheyretmand

Department of Civil Engineering, Faculty of Engineering, Urmia University, Urmia

PAPER INFO

Paper history:

Received 10 February 2020

Received in revised form 20 March 2020

Accepted 19 May 2020

Keywords:

High Strength Rebar

Boundary Element

Shear Wall

Rebar Fracture

Out of Plane Buckling

Crack Width

ABSTRACT

Considering economic reasons and attempting to reduce the carbon footprint of concrete structures, there is an increasing tendency toward the use of high strength reinforcement in seismically active regions. ACI 318-19, Iranian steel rebars standard INSO 3132 and next edition of Iranian national building allow the use of high strength rebars in elements of ductile force-resisting systems. Therefore it is important to verify that if S520 rebars are capable of providing adequate, a) strain capacity, b) out of plane buckling deformation capacity, which are the two common sources of failures observed in recent earthquakes in boundary elements of lightly reinforced shear walls. An experimental program is designed to compare strain capacity of boundary elements reinforced with S400 and S520 rebars, which include monotonic and cyclic loading considering probable loading on lightly reinforced boundary elements. Considering test results for specimens under monotonic and cyclic loading it is shown that, a) gauge length suggested by INSO for rebar test could be misleading in the evaluation of rebar axial strain capacity, b) S520 rebars have limited ductility compared to S400, but considering strain demand, this limited strain capacity is adequate to avoid rebar fracture, c) local strain (crack width) has a better correlation with out of plane buckling compared to average strain as suggested by some researchers, d) it seems that out of plane buckling for S520 rebars occurs at smaller deformation, which means there is the need for larger minimum dimension for sections reinforced with S520 compared to S400.

doi: 10.5829/ije.2020.33.06c.06

NOMENCLATURE

b	Boundary element width (mm)
d_b	Rebar diameter (mm)
f'_c	Concrete compressive strength (MPa)
f_y	Rebar yield stress (MPa)
f_{su}	Rebar ultimate stress (MPa)
h_w	Wall height (mm)
h_{eff}	Wall effective height (mm)
l_{sp}	Strain penetration length (mm)
l_w	Wall length (mm)
R_d	Ductility related modification factor
w_{cr}	Crack width (mm)

Greek Symbols

δ	Element lateral deflection (mm)
ϵ_{fr}	Rebar fracture strain
ϵ_{sm1}	Element strain ignoring strain penetration
ϵ_{sm2}	Element strain evaluated using hardness-strain correlation
μ_ϕ	Median curvature demand in shear walls (1/mm)
ξ	Ratio of lateral deflection to element width
ζ	Critical ratio of lateral deflection to element width
ρ	Reinforcement ratio
σ_ϕ	Standard deviation of curvature demand in shear walls (1/mm)
$\Delta_{r,roof}$	Roof displacement (mm)
Δ_t	Element total elongation (mm)

1. INTRODUCTION

There is a growing tendency toward the use of high strength rebars in reinforced concrete structures in

seismically active regions. The transition to higher strength reinforcement in New Zealand is started as early as 2001, where AS/NZS 4671 in 2001 allowed the use of grade 500E reinforcement instead of grade 430 rebars that is traditionally used in New Zealand for the design of ductile members [1]. This is later incorporated as an amendment to NZS 3101-2006, the New Zealand

*Corresponding Author Institutional Email: s.tariverdilo@urmia.ac.ir (S. Tariverdilo)

code for the design of reinforced concrete structures [2]. AS/NZS 4671 requirements for Grade 500E are given in Table 1.

In the United States, following extensive researches including NIST 14-917-30 and ATC 115; ACI 318-19 allowed the use of ASTM A706 grade 80 in the design of special moment frames and even ASTM A706 grade 100 for special structural walls [3-5]. ASTM A706 grade 60 [6] was already in use for the design of bridge substructures in California (CALTRANS [7]). Table 1 presents the required specification for ASTM A706 grade 80. AS/NZS 4671 and ASTM impose limitation on uniform elongation and total elongation (fracture elongation), respectively. AS/NZS 4671 has lower and upper limitations for the ratio of ultimate to yield strength, while ASTM only requires lower limitation on this ratio.

In Iran, the minimum requirement of INSO 3132 for S520 is very similar to ASTM A706 grade 80, except about elongation requirements [8]. While requirement on elongation for S520 is on $5d_b$ gauge length, A706 requirement is on 200 mm gauge length and as could be seen, INSO's requirement is somewhat relaxed compared to A706.

There are a growing number of researches investigating seismic deformation capacity of different reinforced concrete elements. Rastegarian and Sharifi [9] associated different strain in concrete and steel rebars to different performance levels, used pushover analysis to derive correlation between element drift and objective performance level. Sabrin et al. [10] considered possible variation in concrete ultimate strain and also assumed different plastic hinge length, investigated the adequacy of default plastic hinge properties in ETABS commercial software [10-11]. Linh et al. [12] proposed an experimental setup to study the double curvature test of V shape (L shape) columns using shaking table. They found that the usual assumption of plane strain deformation does not comply with observed behavior in the tests.

Improve modeling and acquiring a better knowledge of the actual response of reinforced concrete shear walls are subjects of different researches [13-15]. Wood [16] analyzed tests on shear walls concluded that walls with longitudinal rebar ratio smaller than 1% could develop limited cracking with very large strain demand on rebars that could lead to its fracture. Dazio et al. [17] developed a comprehensive experimental program to investigate the cyclic response of shear walls. The program includes six large scale specimens with different reinforcement contents and also with reinforcements of different ductility. Test results demonstrated limited cracking in nonlinear deformation zone of shear walls accompanied by premature fracture of longitudinal bars in web or boundary elements (BE) for specimens with a low ratio of longitudinal reinforcement. They also found that only increasing the reinforcement ratio of boundary elements, leads to a limited number of cracking in the web and fracture of web longitudinal reinforcement. Lu et al. [18] conducted experiments on six lightly reinforced shear walls and again concluded that a low ratio of longitudinal bars leads to a small number of cracking in the shear wall and rebar fracture. Latter Lu et al. [19] using finite element models studied the effect of the content of longitudinal bars on the wall cyclic response. They found that desirable response under cyclic loading requires an increase in the ratio of longitudinal rebars in both web and boundary elements. Rosso et al. [20] investigated the cyclic response of thin lightly reinforced boundary elements, with main attention on out of plane buckling of the boundary element, rather than strain profile of the longitudinal bars. They found that rebar ratio and wall thickness are the main parameters controlling the out of plane buckling of thin and lightly reinforced boundary elements. Accounting for these findings, ACI 318-19 has changed the minimum reinforcement requirement for end zones of shear walls. At the same time, NZS 3101-2006 amendment 3 has increased minimum reinforcement for end zones and web of shear walls.

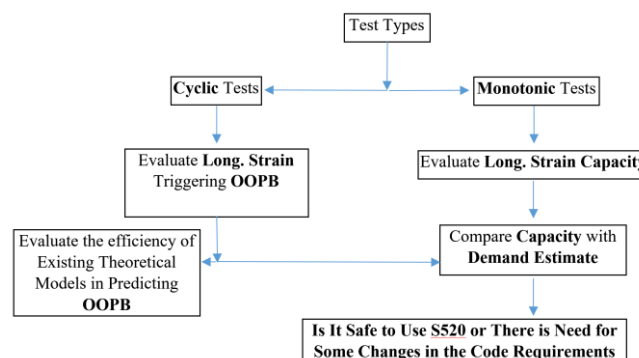


Figure 1. The methodology adopted in this study to evaluate adequacy of S520 rebars

TABLE 1. Different countries code requirement for high strength reinforcement

Reinforcement	Grade 500E	A706 Grade 80	S400	S520
Code	AS/NZS 4671	ASTM A706	INSO 3132	INSO 3132
Actual yield strength (MPa)	500~600	552~676	≥400	520~675
	$5d_b$	-	16	13
Total elongation (%) in	$10d_b$	-	12	-
	200 mm	12	-	-
Uniform elongation (%)	10	-	-	-
Ratio of tensile to yield strength	1.15~1.40	≥1.25	≥1.25	≥1.25
Min. tensile strength (MPa)	-	690	600	690

At the same time, there are improvements in our knowledge of seismic strain demand. Based on numerical analyses on a 13 stories building with a dual lateral force-resisting system, NIST reports a mean strain demand of 1.3% on longitudinal rebars of heavily reinforced BEs [3]. Oztruk [21] showed that the adoption of shear walls in seismic forcing resisting systems could result in a significant reduction of displacement demand and consequently deformation demand on rebars. He also demonstrated that displacement demand in multi-degree of freedom systems could rise by half compared to a single degree of freedom systems with the same period [22].

As discussed in previous paragraphs, the axial strain capacity of longitudinal bars and out of plane buckling controls the seismic response of lightly reinforced BEs. Considering these failure modes, this study developed an experimental program including, a) monotonic tests to mainly evaluate strain capacity of longitudinal bars, and b) cyclic tests to evaluate deformation triggering out of plane buckling (OOPB). Tests are carried out on specimens with S400 and S520 rebars, to assess the adequacy of their ductility for use in BE of ductile shear walls. The cyclic test results are also used to verify the accuracy of available theoretical models predicting out of plane buckling. The Methodology adopted in this study is depicted in Figure 1.

In section 2.1, first some estimates of strain demand on BEs are given. This subsection also discusses how rebar strain after tests are calculated using a correlation between strain and hardness. Finally, this section reviews model predicting axial deformation initiating out of plane buckling. Section 2.2 gives some description of material properties used in the tests, experimental program including specimens information, and loading protocol adopted for cyclic loading. Section 3 discusses experimental results including monotonic tests (section 3.1) and cyclic tests (section 3.2). Finally, in section 3.3 test results are compared with available data provided by other researchers.

2. MATERIALS AND METHODS

2. 1. Demand Estimate, Driving Strain Profile and Model for Prediction of Out of Plane Buckling

To have a better interpretation of the test results, we should have some estimate of strain demand of longitudinal bars in BE. Dezhdar and Adebar [23] conducted extensive numerical analyses on thirteen different buildings with story numbers between 10 and 50, developed an estimate of curvature demand at the base of cantilever shear walls. The estimations include mean ($\mu\phi$) and mean plus one standard deviation ($\mu\phi+\sigma\phi$) of curvature demand as follow:

$$(\mu)_{\phi,\text{demand}} l_w = \left(1.8 - 0.017 \frac{h_w}{R_d} \right) \frac{\Delta_{\text{roof}}}{h_w} \quad (1)$$

$$(\mu + \sigma)_{\phi,\text{demand}} l_w = \left(2.8 - 0.022 \frac{h_w}{R_d} \right) \frac{\Delta_{\text{roof}}}{h_w} \quad (2)$$

where h_w , l_w are wall's height and length, Δ_{roof} is roof displacement and R_d is ductility related force modification factor (usually between 2 and 4.5). For lightly reinforced walls, depth of neutral axis in comparison to wall length is small, consequently tensile strain in BE could be approximated by ϕl_w . Now assuming global drift of 0.02 and setting equal to zero the second terms in the parenthesis, a conservative upper bound evaluation of demand for mean and mean plus one standard deviation will be 0.036 and 0.058, respectively.

Developing strain profile of the rebar after completion of the test is important in the evaluation of rebar fracture. It is known that there is a correlation between hardness and strain for metals [24]. To develop this correlation, uniaxial tensile tests on rebar is interrupted at different plastic strains. Then Rockwell B hardness test is carried out using indent universal hardness test machine on the rebar. Figure 2 shows the Rockwell B hardness test results for rebars (HRB) with different residual strains and the result of a regression analysis carried

out on S400 and S520. To derive the strain profile of the rebar at the end of the test, hardness test is carried out along the rebar length, and using an established correlation between hardness and strain. It is possible to derive the strain profile of the rebar.

Extensive tensile cracking of BEs could lead to instability in the form OOPB of whole specimen rather than buckling of reinforcing bar. Equating moment due to P-Delta with concrete resisting moment in the mid span, Paulay and Prestley [25] found that normalized out of plane displacement ξ should satisfy the following equation:

$$\xi = \frac{\delta}{b} \leq 0.5 \left(1 + 2.35 \frac{\rho f_y}{f_c} - \sqrt{5.53 \left(\frac{\rho f_y}{f_c} \right)^2 + 4.70 \frac{\rho f_y}{f_c}} \right) \quad (3)$$

where δ is mid span lateral deflection, b section dimension and ρ is the ratio of longitudinal reinforcement. Now relating curvature at mid span to strain in the longitudinal reinforcement and using moment area theorem, Paulay and Prestley [25] found that average critical strain triggering OOPB for specimen with one layer of reinforcement is

$$\epsilon_{cr} = 4 \left(\frac{b}{h_w} \right)^2 \xi_{cr} \quad (4)$$

2. 2. Experimental Program BEs of shear walls are under heavy axial loading. Due to the shape of the moment diagram in shear walls. There

is nearly uniform axial force on BE near the wall critical section. Accounting for this nearly uniform axial loading and following Rosso et al. [20] and Haro et al. [26], specimens under uniaxial monotonic and cyclic loading are used to evaluate BE's seismic response. Experimental program includes three monotonic and four cyclic tests with S400 and S520 longitudinal rebars (Table 2). Tests are conducted using a universal jack of 1000 KN capacity in infrastructure research center of Urmia University. Table 2 gives a description of samples considered in the study and Figure 3 depicts the test setup and instrumentation. Three LVDTs and two gauges are used to read axial and lateral deflection of the specimens.

Figure 4 depicts the loading protocol used in the tests. Premature rebar fracture is the primary failure mode in lightly reinforced shear walls. Due to the small ratio of flexural strength to cracking moment, failure is dominated by cracking in concrete rather than compression failure, which could happen only at large drifts. Considering this and following Hilson et al. [27] and Rosso et al. [20], an asymmetric loading protocol is adopted for cyclic loading, which mainly introduces tensile loading on the sample with small compression strain on the order 0.003. Loading protocol is symmetric until reaching a compression strain of 0.003, then protocol becomes asymmetric, where maximum compression strain remains constant, and meanwhile tensile strain increases.

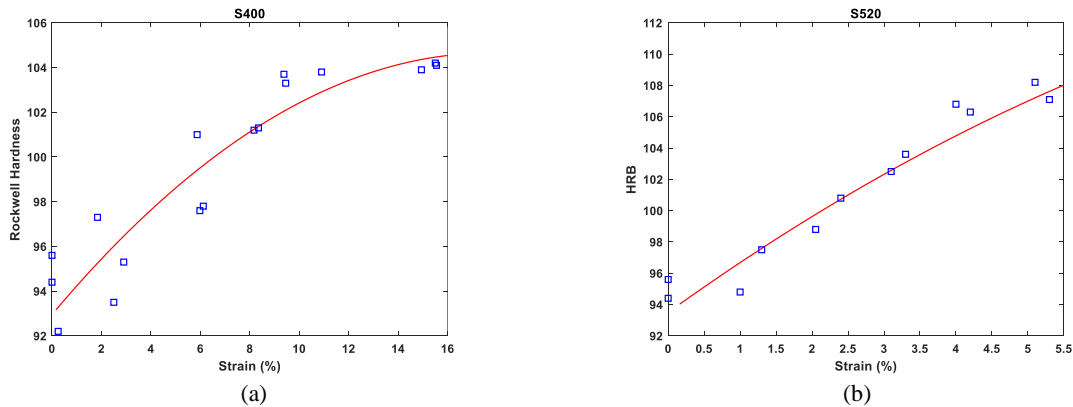


Figure 2. HRB versus residual strain and graph depicting result of regression analysis for, a) S400, b) S520

TABLE 2. Samples description, geometry and reinforcement

Sample Designation	Description	Dim. (mm) $w_1 \times w_2 \times l$	Long. Bar	Rein. Ratio	Trans. Rein.
BM2	S400 Rebar sample 2 under Monotonic loading	150x150x1000	T10	0.00347	T6@150
BM3	S400 Rebar sample 3 under Monotonic loading	"	T10	0.00347	T6@150
BC1	S400 Rebar sample 1 under Cyclic loading	"	T10	0.00347	T6@150
BC2	S400 Rebar sample 2 under Cyclic loading	"	T10	0.00347	T6@150
HM1	S520 Rebar sample 1 under Monotonic loading	"	T10	0.00347	T6@150
HC1	S520 Rebar sample 1 under Cyclic loading	"	T10	0.00347	T6@150
HC2	S520 Rebar sample 2 under Cyclic loading	"	T10	0.00347	T6@150

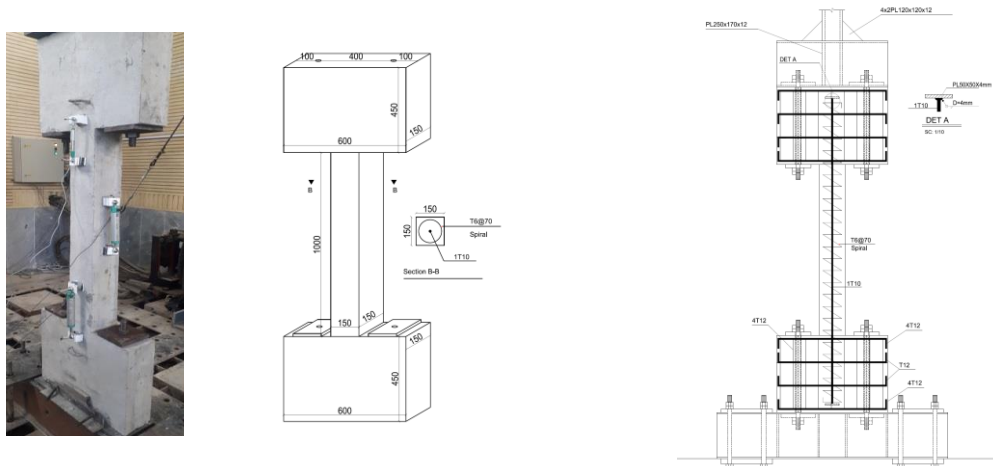


Figure 3. Specimens setup and instrumentation

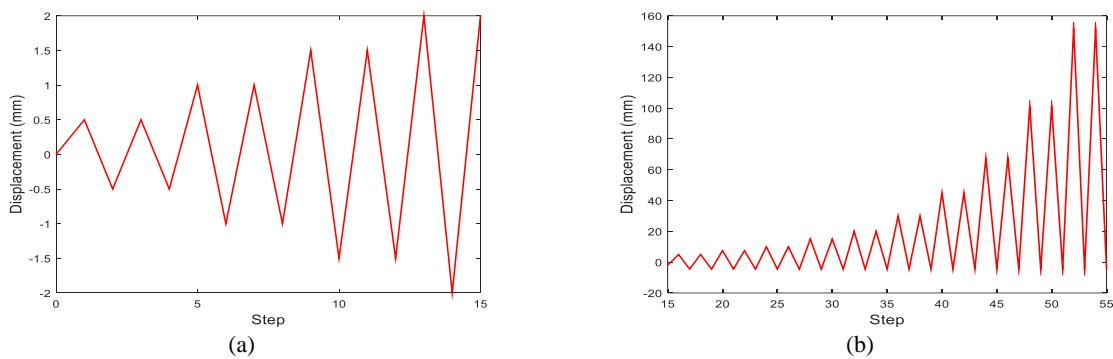


Figure 4. Loading protocol used in the experiments, a) symmetric loading in small displacements, b) asymmetric loading in large displacements

TABLE 3. Material properties for concrete and reinforcements

Designation	Material Property	Reinforcements			
		S400	INSO 3132	S520	INSO 3132
f_y	Yield Stress (MPa)	433	≥ 400	589	$520 \leq f_y \leq 675$
f_{su}	Ultimate Strength (MPa)	622	≥ 600	729	≥ 690
f_{su}/f_y	Ratio of ultimate to yield strength	1.44	≥ 1.25	1.24	≥ 1.25
ϵ_{fr}	Fracture Elongation strain in $5d_b$	0.30	≥ 0.16	0.24	≥ 0.13
	Fracture Elongation strain in $10d_b$	0.27	≥ 0.12	0.15	-
f'_c	Fracture Elongation strain in 200 mm	0.21	-	-	-
	Material Property	Concrete			
	28 days strength (MPa)	30			

Table 3 gives the material properties used in the experiments. Two types of reinforcement are considered in this study including S400 and S520, with specifications similar to ASTM A615 Grade 60 and ASTM A706 grade 80. Reinforcement S520 is acquired from Kavir Steel Complex and is produced using the tempering and quenching process. This table also includes requirements of INSO 3132 for each type of reinforcement.

3. RESULTS

3.1. Monotonic Tests Monotonic tests include two tests on S400 rebar and one test on S520. Figure 5a shows the load-deflection diagrams and Figure 5b gives the cracking pattern of the specimens under monotonic loading.

All tests including S400 and S520 rebars are terminated with rebar fracture at element-foundation

interface or at crack near this interface. A significant increase in the number of cracks is evident for specimens with S520, where seven cracks are developed. In fact cracks 6 and 7 in HM1 are developed just before rebar fracture and test termination. A decrease in total deformation in a move from S400 to S520 is significant. This decrease is also could be seen for fracture elongation in $10d_b$ length in Table 2. Interestingly, in samples with $5d_b$ length, there is no significant reduction in fracture elongation for move from S400 to S520. This shows that ASTM approach in evaluating fracture elongation in 200 mm gauge length is a better reflection of actual deformation capacity of the rebar than INSO's $5d_b$ gauge length.

After test completion, hardness evaluation is carried out on the specimen's rebar and then using correlations established between hardness and strain (Figure 2), strain along the rebar length is back-calculated. In assessing the results of this strain profile, it should be noted that this method cannot capture accurately strain profile near the rebar fracture zone. This means that it is only useful for deriving strain profile at tensile strain about tensile strength, which is the useful range of nonlinear deformation in the rebar. Figure 5 gives the evolution of hardness and axial strain of the specimens BM2 and HM1 along the deformed length, which is slightly larger than undeformed length (1000 mm).

As could be seen, there is a good correlation between strain peaks and crack locations. Due to tension stiffening, rebar strain between cracks reduces to nearly zero. In both specimens, fracture occurs at cracks with the largest hardness along the element length. The maximum strain and ratio of maximum strain to average strain for BM2 are 0.25 and 4.0, and for HM1 are 0.07 and 2.6. Much smaller ratio of maximum to average strain for S520 is mainly due to increase in number of cracking for this reinforcement.

Strain profile could also be used to evaluate strain penetration length (l_{sp}) on either sides of

intermediate cracks. Strain penetration length could be used to find maximum available strain capacity of the rebar at each crack.

Considering strain evolution along the element length in Figure 6, strain penetration length (length at which rebar strain reduces to zero) could be evaluated to be $12d_b$ and $8d_b$. Smaller strain penetration length for S520 is mainly due to its smaller maximum strain compared to S400 (see Table 3 for local strains ε_{sm2}). Altheeb et al. [28] developed an experimental program to derive strain profile of rebar in the vicinity of crack in a notched specimen simulating BE of lightly reinforced shear wall. Their result shows that strain penetration length is at least $9d_b$. At the same time, Patel et al. [29] considering BE of lightly reinforced shear walls, concluded that this length could be approximated to be equal to $3.6d_b$ for rebars with a yield stress of 300 MPa. Using strain penetration length of $12d_b$ and $8d_b$ for S400 and S520 rebars and fracture elongation of rebars with different gauge lengths (Table 4), it is possible to calculate anticipated crack width leading to rebars fracture (not for cracks with strain penetration into foundation). Figure 7 shows the evolution of fracture elongation length with sample length (data taken from Table 4) and crack length (w_{cr}) with rebar length under uniform elongation ($l_{sp}+w_{cr}$). These estimated cracks width corresponding to rebar fracture, could be very useful in assessing damaged elements or post-earthquake reconnaissance.

In Table 4, different estimates of rebar strains are compared for different specimens. As discussed earlier, it is important to have an accurate estimation of the rebars strain on the onset of OOPB and rebar fracture. In this study, different estimates of rebar strain are evaluated as follows:

- 1) Ignoring strain penetration and dividing total elongation (Δ_t) by elements length giving ε_{sm1} .
- 2) Using correlation of hardness-strain to obtaining strain of the rebar after test completion, ε_{sm2} (only applicable for specimens under monotonic loading).

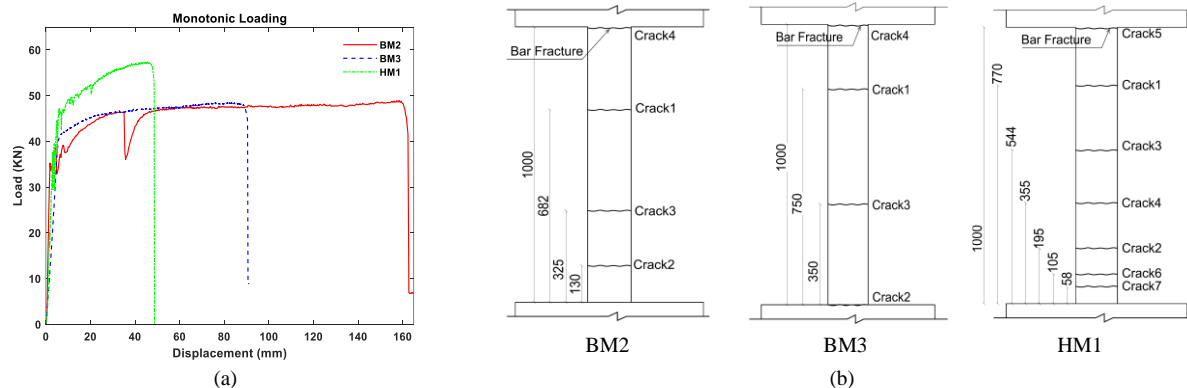


Figure 5. Test results for specimens under monotonic loading, a) load-deflection, b) cracking pattern

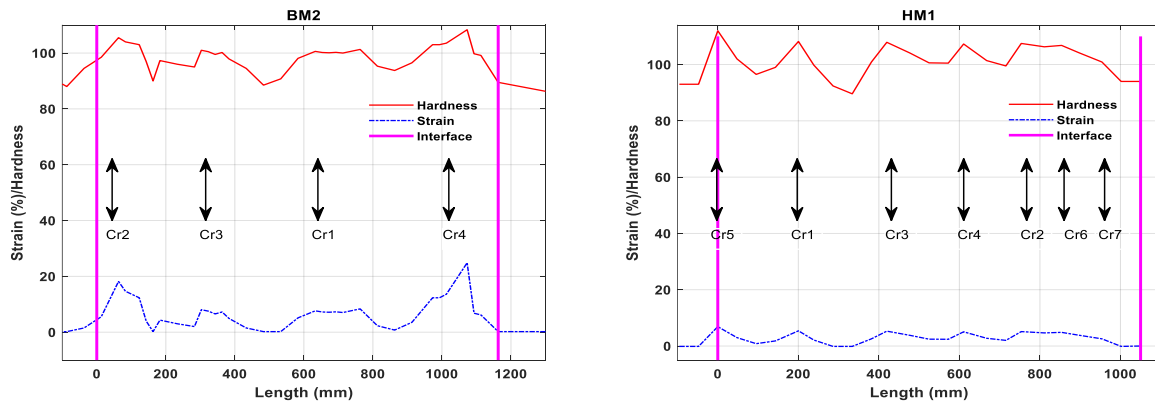


Figure 6. Evolution of Rockwell hardness and axial strain (back calculated from hardness values) with length for specimens under monotonic loading

TABLE 4. Evaluation of average and local strain for specimens under monotonic loading

Sample Designation	Crack Number and Width (mm)							Total Elong. ϵ_{sm1}	Average Strain ϵ_{sm1}	Local Strain ϵ_{sm2}													
										At Each Crack													
										1	2	3	4	5	6	7	1	2	3	4	5	6	7
BM2	1	2	3	4	5	6	7	163	0.163	0.080	0.180	0.080	0.250	-	-	-	1	2	3	4	5	6	7
BM3	31	11	29	20*	-	-	-	91	0.091	0.240	0.170	0.240	0.250	-	-	-	-	-	-	-	-	-	-
HM1	9	5	9	7	13*	5	2	51	0.051	0.054	0.051	0.053	0.050	0.069	0.049	0.026	-	-	-	-	-	-	-

* Bar fracture crack

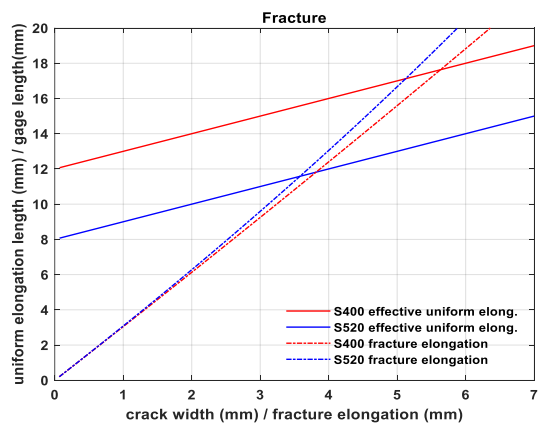


Figure 7. Anticipated crack width corresponding to rebar fracture for S400 and S520

3. 2. Specimens Under Cyclic Loading Two specimens with S400 rebars (BC1 and BC2) and two specimens with S520 rebars (HC1 and HC2) are tested under cyclic loading. Figures 8 and 9 give the load-displacement and cracking pattern of the specimens. Figure 8 is the onset of out of plane buckling for the specimens, which is depicted by an asterisk. Table 5 gives cracking sequences and width for each specimen.

The location of rebar fracture is different for different specimens. While for BC2 and HC2 fracture occur in the element-foundation interface; this happens for BC1 and HC1 along the element length. It is interesting that both of the elements with larger deformation capacity (i.e. BC2 and HC2) has significant strain penetration into foundation.

3. 3. Comparison with Theoretical Models and Other Tests

Dazio et al. [17] in performing experimental investigation on the cyclic response of shear walls concluded that strain capacity on web/boundary element rebars, without/with transverse reinforcement limiting longitudinal bar buckling, are 0.40 and 0.70 of ultimate strain (uniform elongation). An estimate of uniform elongation could be obtained from the monotonic loading of the specimens.

Reviewing test results, the following conclusions could be drawn regarding axial deformation capacity

- **S400.** for monotonic loading 0.091~0.163 and under cyclic one 0.084~0.111, with a ratio of axial deformation capacity in cyclic loading to monotonic one of at least 0.51 (0.084/0.163=0.51).

- S520.** for monotonic loading 0.051 and under cyclic one 0.048~0.060, with a ratio of axial deformation capacity in cyclic loading to monotonic one of at least 0.94 (0.048/0.051=0.94).

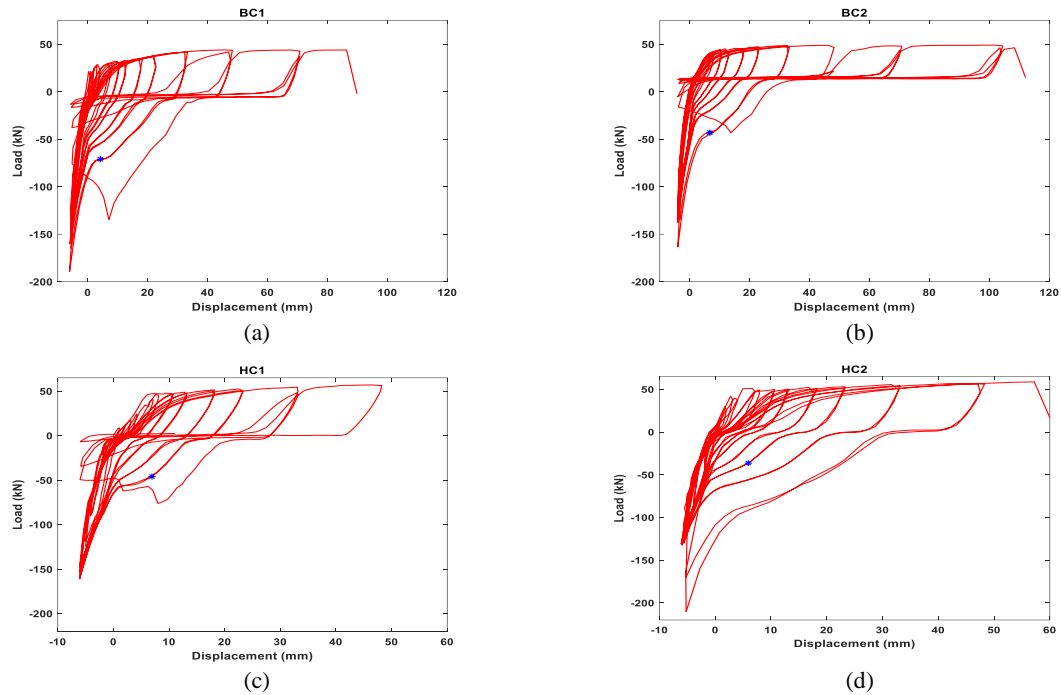


Figure 8. Load-displacement for specimens under cyclic loading, a) BC1, b) BC2, c) HC1, d) HC2

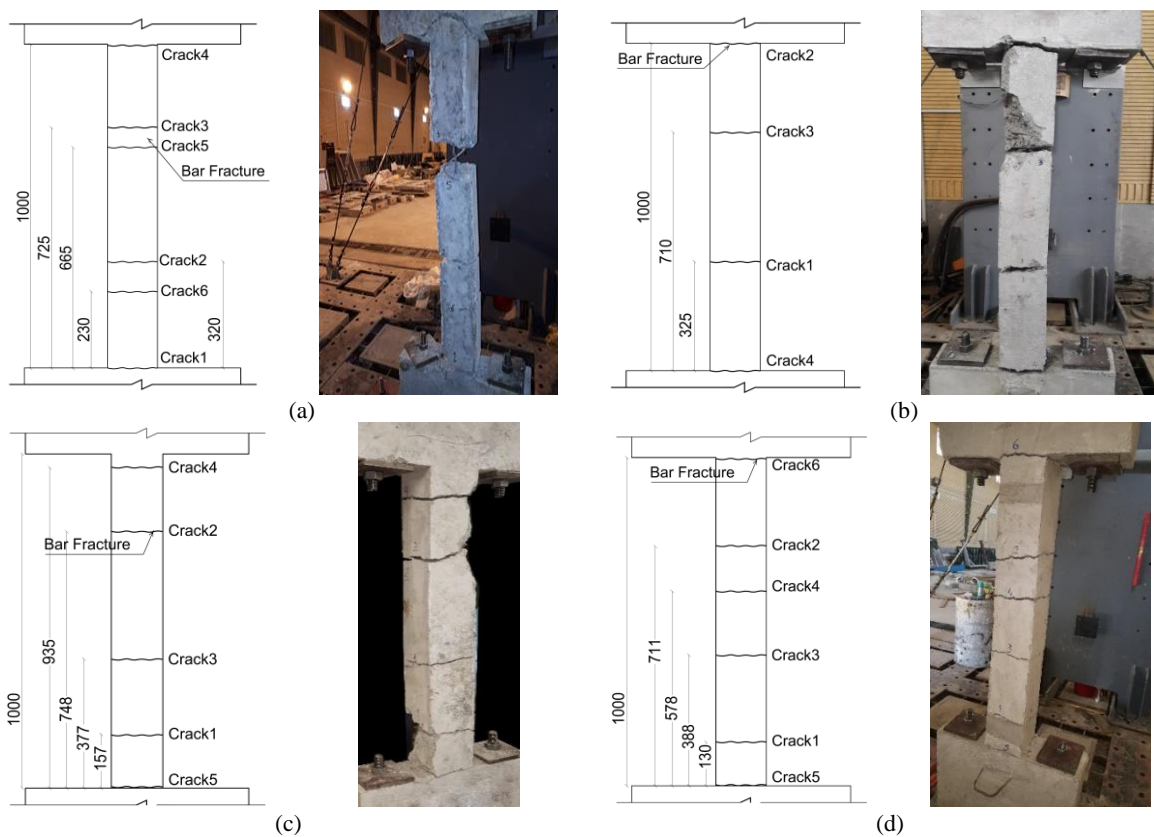


Figure 9. Cracking pattern for specimens under cyclic loading, a) BC1, b) BC2, c) HC1, d) HC2

TABLE 5. Evaluation of strain for specimens under cyclic loading

Sample Designation	Status	Crack Number and Width (mm)						Total Elong.	Aver. Strain ϵ_{sm1}
		1	2	3	4	5	6		
BC1	OOPB	5	4	9**	7	7	-	32	0.032
	Test End	20	19	14*	21	25	12	111	0.111
BC2	OOPB	10**	5	9	8	-	-	32	0.032
	Test End	25	19*	22	18	-	-	84	0.084
HC1	OOPB	4	10**	3	3	-	-	23	0.023
	Test End	8	20*	7	7	6	-	48	0.048
HC2	OOPB	2	3	3	2	2	5**	18	0.018
	Test End	7	11	10	8	8	17*	61	0.060

* Bar fracture crack

** Maximum crack width initiating out of plane buckling

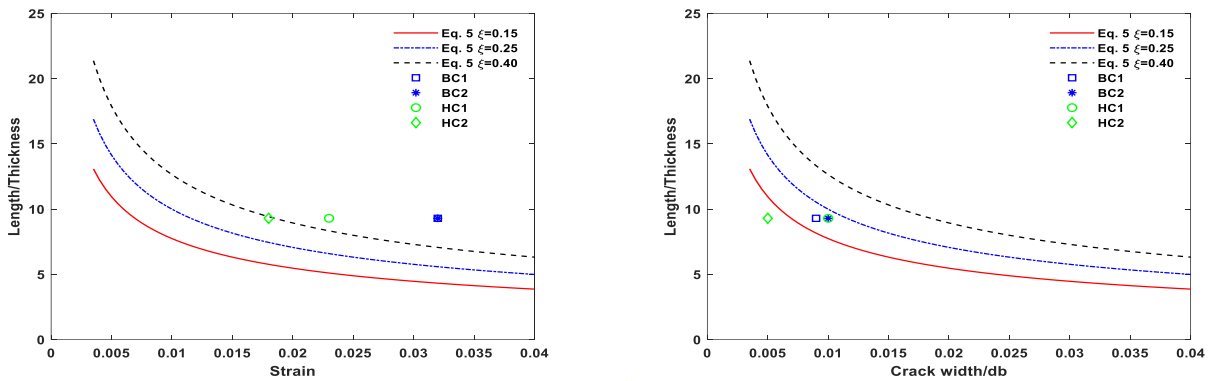


Figure 10. Correlation between bar tensile strain or crack width/ d_b and slenderness ratio of the specimens

As could be seen, the test result in this study conforms well with those of Dazio et al. [17].

An estimate of axial deformation demand could be obtained using Equations (1) and (2) (Dezhdar and Adebar [23]). Using these equations a conservative estimate of strain demand for mean and mean plus one standard deviation are 0.036 and 0.058, respectively. Comparing these estimate for demand with capacities obtained in the tests (at least 0.084 for S400 and 0.048 for S520) shows the adequacy of strain capacity.

A comparison of tensile strain triggering out of plane buckling in tests with predications using Equation (3) (Paulay and Prestley [25]) is prepared in Figure 10. Referring to Table 5, crack width initiating OOPB in specimens with S400 or S520 rebars, are approximately equal. Table 4 also reveals that maximum crack has a better correlation with the onset of out of plane buckling, rather than average axial strain, as suggested by Paulay and Prestley [19]. Accounting for this, Figure 10 depicts the correlation between length/width and average axial strain or crackwidth/ d_b for different samples. Noting that $\zeta=0.25$ usually is associated with lateral deflection initiating OOPB, it could be concluded

that the correlation between crack width and buckling initiation is much stronger than that for average axial strain. This means that the number of cracks as well as total axial deformation is important in any evaluation of vulnerability to out of plane buckling.

Anyway, considering crack width or average axial deformation, it seems that the specimens reinforced with S520 rebars become instable in smaller axial deformations (crack width or average strain). This shows that the minimum section dimension for sections using S520 rebars should be larger than those for S400 rebars.

For elements with a larger ratio of longitudinal reinforcement, the number of cracks increases, and at the same time difference between strain calculated from average strain (ϵ_{sm1}) and local strain (ϵ_{sm2}) that controls crack width decreases. This is also evident for a move from S400 to S520, where a larger number of cracks leads to a more uniform strain profile for S520. This explains why in elements with large reinforcement ratio, good correlation between Equation 5 and average axial strain is reported [26].

4. CONCLUSION

To evaluate the adequacy of S520 for use in lightly reinforced boundary elements, an experimental program including monotonic and cyclic loading is designed. Following results could be established

- Rebar elongation with a gauge length of 5db, as required by INSO, could be misleading. Larger gauge length provides a better estimate of element elongation capacity.
- S520 rebars have limited ductility compared to S400 ones; however, considering anticipated strain demand, strain capacity of S520 could be assessed as adequate.
- Crack width gives a better prediction of out of plane buckling instability compared to average axial strain as suggested by Paulay and Priestley.
- It seems that out of plane buckling in specimens with S520 rebars initiates at smaller deformation compared to the specimens reinforced with S400. This shows the need for an increase in minimum dimension for boundary elements reinforced with S520.

5. REFERENCES

1. Australia/New Zealand Standard 4671, "Steel reinforcing materials, AS/NZS 4671:2001", Sydney, Australia/Wellington, New Zealand, (2001).
2. NZS Standard 3101, "Concrete structures standard, NZS 3101:2006, Amendment 3", Wellington, New Zealand, (2017).
3. NIST 14-917-30, 2014, "Use of High-Strength Reinforcement in Earthquake-Resistant", Concrete Structures, GCR 14-917-30, prepared by the NEHRP Consultants Joint Venture, a partnership of the Applied Technology Council and the Consortium for Universities for Research in Earthquake Engineering, for the National Institute of Standards and Technology, Gaithersburg, Maryland, (2014).
4. ACI 318-19., "Building Code Requirements for Structural Concrete and Commentary, ACI 318-19", ACI Committee 318, American Concrete Institute, Farmington Hills, Michigan, (2019), DOI: 10.14359/51716937.
5. ATC 115, "Roadmap for the use of high-strength reinforcement in reinforced concrete design", Applied Technology Council, Redwood City, California, (2014).
6. ASTM A706, "Standard Specification for Low-Alloy Steel Deformed and Plain Bars for Concrete Reinforcement, ASTM A706-09", ASTM International, West Conshohocken, Pennsylvania, (2009).
7. CALTRANS, "CALTRANS seismic design criteria", version 1.7, California, (2013).
8. INSO 3132. "Hot – rolled steel bars for reinforcement of concrete, Specification and test methods", Iranian National Standardization Organization, Iran, (2013).
9. Rastergarian, S., Sharifi, A., "An investigation on the correlation of inter-story drift and performance objectives in conventional RC Frames", *Emerging Science Journal*, Vol. 2, No. 3, (2018), 140-147.
10. Sabrin, R., Siddique, M.A., Sohel, Md.K., "Seismic performance assessment of existing RC frames with different ultimate concrete strains", *Civil Engineering Journal*, Vol. 4, No. 6, (2018), 1273-1287.
11. ETABS, "Integrated building design software", Computers and Structures Incorporation, California, (2016).
12. Linh, N.N., Hung, N.V., Huy, N.X., "Double curvature test of reinforced concrete columns using shaking table: A new test setup", *Civil Engineering Journal*, Vol. 5, No., 9, (2019), 1863-1876.
13. Tariverdilo, S., Farjadi, A., Barkhordary, M., "Fragility curves for reinforced concrete frames with lap spliced columns", *International Journal of Engineering, Transactions A, Basics*, Vol. 22, No. 3, (2009), 213-224.
14. Asgari, M., Tariverdilo, "Investigating the seismic response of structural walls using nonlinear static and incremental dynamic analyses", *International Journal of Engineering, Transactions B*, Vol. 30, No. 11, (2017), 1694-1699.
15. Heydari, M., Behnamfar, F., Zibasokhan, H., "A macro-model for nonlinear analysis of 3D reinforced concrete shear walls", *International Journal of Engineering, Transactions B, Applications*, Vol. 31, No. 2, (2018), 220-227.
16. Wood, S.L., "Minimum tensile reinforcement requirements in walls." *ACI Structural Journal*, Vol. 86, No. 5, (1989), 582-591.
17. Dazio, A., Beyer, K., Bachmann, H., "Quasi-static cyclic tests and plastic hinge analysis of RC structural walls", *Engineering Structures*, Vol. 31, (2009), 1556-1571.
18. Lu, Y., Henry, R.S., Gultom, Ma, Q.T., "Experimental testing and modelling of reinforced concrete walls with minimum vertical reinforcement", NZSSE Conference, New Zealand, (2015).
19. Lu, Y., Henry, R.S., "Comparison of vertical reinforcement requirements for reinforced concrete walls", *ACI Structural Journal*, Vol. 115, No. 3, (2018), 673-687.
20. Rosso, A., Jimenez-Roa, L.A., Almeida, J.P., Blando, C.A., Bonett, R.L., Beyer, K., "Cyclic tensile-compressive tests on thin concrete boundary elements with a single layer of reinforcement prone to out-of-plane instability", *Bulletin of Earthquake Engineering*, Vol. 16, (2018), 859-887.
21. Ozturk, B., "Investigation of seismic behavior of reinforced concrete shear wall building frames subjected to ground motions from the 1999 Turkish earthquakes", 14th World Conference on Earthquake Engineering, (2008).
22. Ozturk, B., "Seismic Drift Response of building structures in seismically active and near-fault regions", PhD Dissertation, Purdue University, Indiana, US, (2003).
23. Dezhdar, E., Adebar, P., "Estimating seismic demand on concrete shear wall buildings", 11th Canadian Conference on Earthquake Engineering, (2012).
24. Loporcario, G., Pampanin, S., Kral, M.V., "Investigating the relationship between hardness and plastic strain in reinforcing steel bars", NZSEE Conference New Zealand, (2014).
25. Paulay, T., Priestley, M.J.N., "Seismic design of reinforced concrete and masonry building", John Wiley and Sons, 744. (1992).
26. Haro, A.G., Kowalsky, M., Chai, Y.H., Luciera, G.W., "Boundary Elements of Special Reinforced Concrete Walls Tested under Different Loading Paths", *Earthquake Spectra*, Vol. 34, No. 3, (2018), 1267-1288
27. Hilson, C.W., Segura, C.L., Wallace, J.W., "Experimental study of longitudinal reinforcement buckling in reinforced concrete structural wall boundary element", Tenth U.S. National Conference on Earthquake Engineering: Frontiers of Earthquake Engineering, Anchorage Alaska, (2014), DOI: 10.4231/D3CC0TT9C.

28. Altheeb, A., Albidah, A., Lam, N.T.K., Wilson, J., "The development of strain penetration in lightly reinforced concrete shear walls", Australian Earthquake Engineering Society 2013, Hobart Tasmania, (2013).
29. Patel, V.J., Van, B.C., Henry, R.S., Clifton, G.C., "Effect of reinforcing steel bond on the cracking behavior of lightly reinforced concrete members", *Construction and Building Materials*, Vol. 96, No. 2, (2015), 238–247.

Persian Abstract

چکیده

مباحث اقتصادی و کاهش آلاینده‌گی از دلایل اصلی اقبال به آرماتورهای مقاومت بالا در سال‌های اخیر تلقی می‌شوند. از طرفی پیشرفت‌های تکنولوژیک نیز این امکان را فراهم آورده است که علیرغم افزایش مقاومت، آرماتورهای مقاومت بالا دارای شکل‌پذیری مناسبی باشند. با در نظر گرفتن موارد فوق آئین‌نامه ACI 318-19 و اصلاحیه شماره ۳ آئین‌نامه NZS 3101-2006، اجازه استفاده از آرماتورهای مقاومت بالا را در اجزا باربر لرزه‌ای داده‌اند. در ایران ویرایش آتی مبحث ۹ مقررات ملی ساختمان نیز اجازه استفاده از آرماتور S520 را داده است. از سویی طلب کرنشی بالایی روی اجزا مرزی دیوارهای برشی با آرماتور طولی اندک وجود دارد که منجر به خرابی‌های مکرری در زلزله‌های اخیر شده است. با توجه به این طلب کرنشی بالا، تعیین کفایت S520 برای کاربرد به عنوان آرماتور طولی المان مرزی مهم خواهد بود. برای بررسی این امر برنامه آزمایشگاهی در بر گیرنده آرماتورهای S400 و S520 تدوین شد که شامل نمونه‌های تحت بار محوری یکنوا و رفت و برگشتی است. نتایج آزمایشات نشانگر موارد زیر بوده است: الف) تخمین ارائه شده با آزمایش روی آرماتور با طول $5d_b$ می‌تواند به تخمین نادرستی از ظرفیت کرنشی اجزا لرزه‌ای ختم شود، ب) نمونه‌های با آرماتور S520 دارای شکل‌پذیری کمتری در قیاس با S400 هستند، ولی کماکان با در نظر گرفتن طلب کرنشی محتمل برای کاربرد لرزه‌ای مناسب می‌باشند، پ) عرض ترک در قیاس با کرنش متوسط همبستگی بهتری با شروع کمانش دارد، ت) کرنش کششی متناظر شروع کمانش المان برای S520 کمتر است، این امر نشانگر نیاز به افزایش بعد حداقل المان مرزی برای این آرماتور است.
